Biotic manganese oxidation coupled with methane oxidation using a continuous-flow bioreactor system under marine conditions

Shingo Kato, Masayuki Miyazaki, Sakiko Kikuchi, Teruhiko Kashiwabara, Yumi Saito, Eiji Tasumi, Katsuhiko Suzuki, Ken Takai, Linh Thi Thuy Cao, Akiyoshi Ohashi and Hiroyuki Imachi

ABSTRACT

Biogenic manganese oxides (BioMnOx) can be applied for the effective removal and recovery of trace metals from wastewater because of their high adsorption capacity. Although a freshwater continuous-flow system for a nitrifier-based Mn-oxidizing microbial community for producing BioMnOx has been developed so far, a seawater continuous-flow bioreactor system for BioMnOx production has not been established. Here, we report BioMnOx production by a methanotroph-based microbial community by using a continuous-flow bioreactor system. The bioreactor system was operated using a deep-sea sediment sample as the inoculum with methane as the energy source for over 2 years. The BioMnOx production became evident after 370 days of reactor operation. The maximum Mn oxidation rate was 11.4 mg L^{-1} day^{-1}. An X-ray diffraction analysis showed that the accumulated BioMnOx was birnessite. 16S rRNA gene-based clone analyses indicated that methanotrophic bacterial members were relatively abundant in the system; however, none of the known Mn-oxidizing bacteria were detected. A continuous-flow bioreactor system coupled with nitrification was also run in parallel for 636 days, but no BioMnOx production was observed in this bioreactor system. The comparative experiments indicated that the methanotroph-based microbial community, rather than the nitrifier-based community, was effective for BioMnOx production under the marine environmental conditions.

Key words | biogenic manganese oxides, continuous-flow bioreactor system, manganese-oxidizing bacteria, metal recovery, methanotroph, nitrifier

Shingo Kato
Sakiko Kikuchi
Teruhiko Kashiwabara
Katsuhiko Suzuki
Ken Takai
Ore Genesis Research Unit, Project Team for Development of New-generation Research Protocol for Submarine Resources,
Japan Agency for Marine-Earth Science and Technology (JAMSTEC),
Yokosuka,
Kanagawa 237-0061, Japan

Shingo Kato
Sakiko Kikuchi
Teruhiko Kashiwabara
Katsuhiko Suzuki
Ken Takai
Hiroyuki Imachi (corresponding author)
Research and Development Center for Submarine Resources,
JAMSTEC,
Yokosuka,
Kanagawa 237-0061, Japan
E-mail: *imachi@jamstec.go.jp*

Masayuki Miyazaki
Yumi Saito
Eiji Tasumi
Ken Takai
Hiroyuki Imachi
Department of Subsurface Geobiological Analysis and Research (D-SUGAR),
JAMSTEC,
2-15 Natsuhima-cho,
Yokosuka,
Kanagawa 237-0061, Japan

Linh Thi Thuy Cao
Akiyoshi Ohashi
Department of Civil and Environmental Engineering,
Graduate School of Engineering,
Hiroshima University,
Higashi-Hiroshima,
Hiroshima 739-8511, Japan

INTRODUCTION

Mn(IV) oxyhydroxides (hereafter, Mn oxides) are ubiquitous absorbents of various elements in aquatic environments (Dixon & Skinner 1992; Manceau *et al.* 1992; Post 1999; Takahashi *et al.* 2007; Sherman & Peacock 2010; Kashiwabara *et al.* 2011, 2013, 2014). In particular, marine ferromanganese crusts and nodules, which are massive deposits of Mn oxides widely found on the deep seafloor, have received great attention as potential metal resources

doi: 10.2166/wst.2017.365

because of their strong enrichment of many valuable metals from seawater (Glasby 2006; Hein *et al.* 2013).

Mn oxidation in the natural environment is believed to be dominated by biological activity (Myers & Nealson 1988; Tebo *et al.* 2004). A diverse array of bacteria and fungi are known to be Mn oxidizers (Tebo *et al.* 2005; Templeton *et al.* 2005; Miyata *et al.* 2006; Santelli *et al.* 2011). Biological Mn oxidation is induced by Mn-oxidizing enzymes (i.e., multicopper oxidases) (van Waasbergen *et al.* 1996; Dick *et al.* 2008; Tebo *et al.* 2010) or by superoxides as byproducts of metabolisms (Hansel *et al.* 2012; Learman *et al.* 2013). Biogenic Mn oxides (hereafter BioMnOx) have a greater reactivity than abiotic forms due to the larger surface area accompanied by their smaller size, the more vacancies for cations associated with their crystal structures, and the greater chemical complexity with coexisting organics (Hochella *et al.* 2008). Because of their structural and chemical properties, BioMnOx absorb significant amounts of trace metals such as Ni and Co that are normally present at low levels in the environments and are economically valuable elements (Tebo *et al.* 2004, 2010; Miyata *et al.* 2007; Hennebel *et al.* 2009). Therefore, BioMnOx have been studied regarding engineering applications such as the recovery of trace metals from wastewater and remediation of groundwater contaminated with toxic metals (Hennebel *et al.* 2009).

Recently, the use of a continuous-flow system called down-flow hanging sponge (DHS) bioreactor for continuous Mn removal and BioMnOx production under freshwater conditions has been reported (Cao *et al.* 2015). In this report, BioMnOx production coupled with nitrification was successful with no supply of organic matter. In the presence of high concentrations of organic compounds, on the other hand, BioMnOx production was not observed (i.e., no Mn-oxidizing microbes could be cultivated), suggesting that the nitrifier-derived organic compounds seem to be essential for BioMnOx production and the development of potentially oligotrophic Mn-oxidizing microbial populations. In addition, Cao *et al.* (2015) reported the effective removal of trace metals such as Ni and Co with the Mn precipitation. These results indicate a great potential for BioMnOx production using the DHS bioreactor system over conventional batch incubation systems because this system can effectively combine the continuous precipitation of Mn and recovery of trace metals from the influent.

The mass of seawater is much greater (over 97% of the total water mass on the Earth) than that of freshwater. If BioMnOx production using a continuous-flow system can be achieved under marine conditions, there is the possibility of recovering trace metals (such as Ni and Co) continuously from seawater. Although numerous studies on recovery of metals including Ni and Co from seawater have been reported (reviewed in Diallo *et al.* (2015)), no continuous-flow bioreactor system for BioMnOx production and metal recovery has been established under marine conditions to date. Here, we report Mn removal and BioMnOx production during the long-term operation (over 2 years) of a DHS reactor under marine conditions. To this end, according to the cultivation strategy reported previously (Cao *et al.* 2015), we attempted to cultivate marine Mn-oxidizing microorganisms coupled with nitrification in a reactor system amended with ammonium, in which soluble microbial organic products were provided by nitrifiers to concurrent Mn oxidizers as the substrates. We also set up another DHS bioreactor to cultivate Mn oxidizers coupled with methane oxidation instead of nitrification. We were only able to successfully enrich a BioMnOx-producing microbial community from a deep-sea sediment sample with the methane-fed DHS bioreactor. In addition, the methanotroph-based microbial community capable of BioMnOx production during the enrichment was characterized.

MATERIALS AND METHODS

DHS reactors and their operational conditions

We operated two DHS reactors, namely reactors A and M. For reactor A, ammonium (NH_4^+) was provided as the sole energy source. In contrast, methane (CH_4) was used as the energy source for reactor M. NH_4^+ and nitrate (NO_3^-) were also provided to reactor M as nitrogen sources (described below). The DHS reactors used in the present study (Figure 1) are similar to a previously described model (Cao *et al.* 2015). The DHS bioreactors have strings of 22 cubic polyurethane sponges ($2 \times 2 \times 2$ cm, pore size of 0.83 mm) connected diagonally in series and hung in a closed polyvinyl chloride (PVC) column (inside volume, 1.07 L). The total volume of the sponges was 0.176 L, and this volume was used for calculating the hydraulic retention time (HRT) and the gas retention time (GRT). The initial GRT for each reactor operation was determined based on the calculation of chemical oxygen demand of NH_4^+ or CH_4. The column of reactor M was replaced with a larger PVC column (inside volume, 3.085 L) at a time of 634 days of operation, because large biofilms that grew on three sponge cubes from the top reached the inner wall of the column, and thus some of the medium went

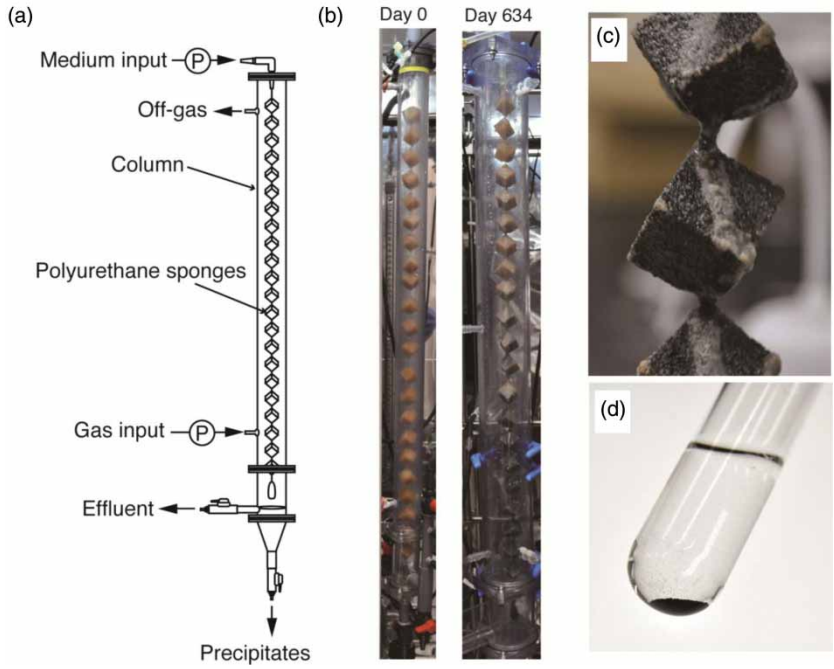

Figure 1 | DHS reactor used in the present study. (a) Schematic diagram of the DHS reactor. (b) Photographs of the DHS reactor with methane (reactor M; see text for details) on days 0 and 634. On day 634, sponges at the lower portion of the reactor became blackish. (c) An enlarged photograph of the sponges at the lower potion on day 634. Blackish BioMnOx (biogenic Mn oxides) and whitish microbial mats were observed on the sponges. (d) A photograph of BioMnOx collected from the sponges on day 634.

down along the inner wall without passing through the sponge cubes.

We used a deep-sea sediment sample, which was collected from the Tarama Knoll, southern Okinawa Trough, Japan (25°5.576′N, 124°32.377′E), at a depth of 1,540 m, by the remotely operated vehicle *Hyper-Dolphin* (cruise NT10-06, dive no. 1108, April 10, 2010) (Makita *et al.* 2016), as the inoculum for the operation. Just before the operation of reactors A and M, the sponge cubes were soaked in a suspension of the sediment sample (Figure S1, available with the online version of this paper). It is noted that NH_4^+ and CH_4 were detected in the seawater and shimmering fluid samples obtained from the Tarama Knoll (Yamanaka *et al.* 2015). Following the inoculation, the PVC columns were tightly closed and installed in an incubation chamber (M-600FN, Taitech, Koshigaya, Japan) in the dark at 15 °C.

The operational conditions used in this study are summarized in Table 1. The composition of the medium was as follows (L^{-1}, the values for x were adjusted at each operation phase; see Table 1): x g $MnCl_2{\cdot}4H_2O$, x g $(NH_4)_2SO_4$, x g KNO_3, 0.04 g KH_2PO_4, 1.33 g $CaCl_2{\cdot}4H_2O$, 3.4 g $MgSO_4{\cdot}7H_2O$, 4.18 g $MgCl_2{\cdot}6H_2O$, 0.33 g KCl, 24 g NaCl, 0.084 g $NaHCO_3$, 1 mL trace mineral element solution, and 1 mL vitamin solution. The trace mineral element solution contained the following (L^{-1}): 2.5 g EDTA·2Na, 5 g $MnSO_4{\cdot}2H_2O$, 5 g $CoSO_4{\cdot}7H_2O$, 1.8 g $ZnSO_4{\cdot}7H_2O$, 0.1 g $CuSO_4{\cdot}5H_2O$, 0.2 g $KAl(SO_4)_2{\cdot}12H_2O$, 0.1 g H_3BO_3, 0.01 g $Na_2MoO_4{\cdot}2H_2O$, 0.1 g $SrCl_2{\cdot}6H_2O$, 0.1 g NaBr, 0.1 g KI, 1 g $FeCl_2{\cdot}4H_2O$, 0.25 g $NiCl_2{\cdot}6H_2O$, 0.0017 g Na_2SeO_3, and 0.0033 g $Na_2WO_4{\cdot}2H_2O$. The vitamin solution was composed of the following vitamins (L^{-1}): 2 mg biotin, 2 mg folic acid, 10 mg pyridoxine hydrochloride, 5 mg thiamine hydrochloride, 5 mg riboflavin, 5 mg nicotinic acid, 5 mg DL-calcium pantothenate, 0.1 mg vitamin B_{12}, 5 mg *p*-aminobenzoic acid, and 5 mg lipoic acid. The salinity of the medium showed 3.55%, which is the same level of that of natural seawater. Although we did not measure the salinity of the original sediment samples, the salinity level is probably very similar to that of natural seawater. The pH of the medium was adjusted to 7 or 7.5. A total of 10 L of medium was made at a time. The 10 L medium bottle was stored at 15 °C in the sample incubation chamber. The influent medium was supplied into the reactor column from the top inlet port by a peristaltic pump (Masterflex L/S tubing pump 7550-50, Cole-Parmer, Vernon Hills, IL, USA). The medium then flowed down, passing through the sponge cubes by gravity, and was finally pumped out of the PVC column. The sponge cubes were not submerged, and hung freely in the atmosphere. Air (for reactor A) or a gas mixture of air and CH_4 (final 2% or 4% of CH_4, for reactor M) was

Table 1 | Operational conditions for the DHS reactors

Phase	Operation time (days)	Interval time (days)	Mn^{2+} (μM)	NH_4^+ (μM)	NO_3^- (μM)	pH	CH_4 (%)	HRT[a] (hrs)	GRT[b] (hrs)
Operation with NH_4^+ (reactor A)									
1	0–77	77	118	363	–	7	–	4.5	192
2	78–161	83	118	363	–	7	–	4.5	192
3	162–168	6	118	363	–	7	–	2.3	96
4	169–258	89	118	182	–	7	–	2.3	96
5	259–370	111	118	182	–	7.5	–	2.3	96
6	371–532	161	27	182	–	7.5	–	2.3	96
7	533–636	103	27	182	–	7.5	–	4.5	96
Operation with CH_4 (reactor M)									
1	0–71	71	118	363	297	7	2	4.5	22.5
2	72–196	124	118	36	297	7	2	4.5	22.5
3	197–210	13	118	36	297	7	2	4.5	11.3
4	211–231	20	118	36	297	7	4	4.5	11.3
5	232–258	26	118	36	0	7	4	4.5	11.3
6	259–341	82	118	36	0	7.5	4	4.5	11.3
7	342–370	28	118	36	0	7.5	4	4.5	5.6
8	371–559	188	27	36	297	7.5	4	4.5	2.8
9	560–587	27	27	0	297	7.5	4	4.5	2.8
10	588–746	158	27	36	297	7.5	4	4.5	2.8

[a]Hydraulic retention time.
[b]Gas retention time.

packed into an aluminum bag (AAK-10, ASONE, Osaka, Japan) and supplied to the lower part of the bioreactor column via a peristaltic pump. The medium and gases were supplied intermittently at 1 min/9 min (on/off) regulated by an automatic on/off timer (FT-011, Tokyo Glass Kikai Co. Ltd, Tokyo, Japan) connected to the peristaltic pump. The HRT and GRT were changed by altering the flow rate of the peristaltic pump. The bioreactors were operated under atmospheric pressure.

Chemical analysis of influent and effluent samples

The influent and effluent were routinely sampled to characterize the chemical composition of the medium related to Mn(II) oxidation. Prior to analysis, all the water samples were filtered using 0.22-μm pore size polyvinylidene difluoride membrane filter discs (Merck Millipore, Darmstadt, Germany). The dissolved Mn(II) was measured with the periodate oxidation method using a Hach water quality analyzer (DR-2500; Hach Co., Loveland, CO, USA). NH_4^+-N concentration was determined by the Nessler method using the DR-2500 Hach water quality analyzer. Concentrations of NO_2^--N and NO_3^--N were measured by high-performance liquid chromatography using a TSKgel SAX column (Tosoh Co., Shunan, Japan; eluent, 1.0 N NaCl; column temperature was room temperature) and a UV-VIS detector (GL-7451; GL Science, Tokyo, Japan), as described previously (Maruo *et al.* 2006). Concentrations of CH_4 and CO_2 in the off-gas were determined by gas chromatography (GC3200G; GL Science) with a thermal conductivity detector. O_2 concentrations in the off-gas were monitored using an oxygen concentration meter (JKO-25LII; JIKCO, Tokyo, Japan) that was installed on the off-gas line. The pH of the influent and effluent water was measured using a portable pH meter (Five Go FG2; Mettler Toledo, Columbus, OH, USA).

Identification of Mn oxides

Blackish materials produced on the sponges were collected, freeze-dried, and powdered using an agate mortar. The resultant powders were mounted on a glass holder and analyzed using an X-ray diffraction (XRD) analyzer (MiniflexII, Rigaku Co., Tokyo, Japan) with Cu Kα radiation operated

at 30 kV, 15 mA. Signals were collected from 3° to 90° (2θ) with a scan speed of 4.0° min^{-1} and a scan step of 0.02°.

16S rRNA gene analysis

Genomic DNA was extracted from several sponge cubes randomly selected from two or three portions of the upper, middle, and lower parts of the DHS reactors and the original inoculum. The 16S rRNA gene clone analysis was performed as previously described (Imachi *et al.* 2011). In brief, bacterial and archaeal 16S rRNA genes were amplified by polymerase chain reaction (PCR) with the EUB338F*/1492R and Arc21f/Ar912R primer sets, respectively. The PCR products were cloned, and randomly selected clones (approximately 100 clones for each library) were sequenced. Based on the 16S rRNA gene sequences, OTUs (operational taxonomic units) were defined at a 97% similarity level, and the coverage for each library and number of OTUs shared among the libraries were calculated using mothur 1.36.1 (Schloss *et al.* 2009). The potential microbial community structures based on the 16S rRNA gene phylotype compositions were determined using QIIME 1.9.1 (Caporaso *et al.* 2010). The sequences of representative clones for the OTUs, and relatives of environmental clones and cultured species were aligned using Muscle version 3.8.31 (Edgar 2004). Gap positions were removed from the alignment using TrimAl version 1.2 (Capella-Gutierrez *et al.* 2009). Using the alignment without gaps, phylogenetic trees were constructed using FastTree version 2.1.7 (Price *et al.* 2010) with the Jukes–Cantor nucleotide substitution model. The 16S rRNA gene sequences reported in this study have been deposited in the DNA Data Bank of Japan under accession numbers LC140542–LC140671.

Quantitative real-time PCR (Q-PCR) was performed using SYBR Green I fluorescent dye as previously described (Aoki *et al.* 2014). The numbers of cells were estimated from the Q-PCR results based on the averages of 4.12 copies $cell^{-1}$ for bacteria and 1.63 copies $cell^{-1}$ for archaea, respectively, reported in a curated database of ribosomal RNA operons (rrnDB) version 4.4.4 (Stoddard *et al.* 2015).

Electron microscopy

To obtain scanning electron microscopy (SEM) images of microbial cells attached to the sponges, a portion of a sponge was prefixed in 2.5% (w/v) glutaraldehyde in filtered artificial seawater (FASW) at 15 °C. After being cut with a cleaned blade, and washed in FASW, the sponges were stuck on a poly-L-lysine-coated glass slide for 30 min at room temperature. Following this treatment, the sponges were fixed in 2% (w/v) osmium tetroxide dissolved in FASW. After the samples were rinsed with distilled water, conductive staining was performed by incubation with 0.2% aqueous tannic acid (pH 6.8) for 30 min, and the samples were then washed with distilled water and treated with 1% aqueous osmium tetroxide for 1 hour. After that, the samples were dehydrated in a graded ethanol series and critical-point-dried in a JEOL JCPD-5 (Tokyo, Japan). The samples were coated with osmium using an osmium plasma coater (POC-3; Meiwafosis Co., Ltd, Tokyo, Japan) and observed with a JEOL JSM-6700F field emission scanning electron microscope operated at 5 kV.

RESULTS AND DISCUSSION

Operation of DHS bioreactor supplemented with NH_4^+ (reactor A)

Following a previous report of BioMnOx production using a DHS reactor under freshwater conditions with NH_4^+ as the sole energy source (Cao *et al.* 2015), we attempted to establish BioMnOx production using a DHS reactor under seawater conditions with NH_4^+. To determine the appropriate cultivation conditions for the BioMnOx-producing microbial community, we altered the Mn^{2+} and NH_4^+ concentrations and pH of the influent medium and the HRT and GRT at each operation phase (1 to 7; Table 1). We started the operation of the DHS reactor with an influent containing 118 μM (=6.5 mg L^{-1}) Mn(II) and 363 μM NH_4^+-N at an HRT of 4.5 h. In phase 1 (particularly the last part of the phase), the pH value of the effluent dramatically decreased from 7.0–7.2 to 6.3 (Figure S2, available with the online version of this paper) due to the following reaction of ammonium oxidation:

$$NH_4^+ + 1.5O_2 \rightarrow NO_2^- + H_2O + 2H^+ \quad (1)$$

The decrease in NH_4^+ was stoichiometrically consistent with the increase in NO_2^- (Figure S2). It has been reported that a neutral or an alkaline pH is favorable for chemical and biological Mn(II) oxidation (Hallberg & Johnson 2005). Therefore, to prevent the decrease in pH in the medium by nitrification, a Good's buffer of 3-morpholinopropanesulfonic acid (MOPS) was added into the influent medium at phase 2. Active ammonium oxidation was observed continuously through phase 2, but the pH value in the effluent was maintained around 6.8. However, Mn(II) removal was not observed in phase 2. In addition,

the Mn^{2+} concentrations in the effluent were higher than those in the influent. The reason for this difference is not clear, but the MOPS buffer might affect the variation of Mn^{2+} concentrations in the effluent. Therefore, the addition of MOPS was stopped at the end of phase 2.

In phase 3, the HRT and GRT were shortened. Sequentially, in phase 4, the NH_4^+ concentration in the medium was reduced to half of the initial concentration to prevent the pH decrease. During the operation of phase 4, almost all ammonium was completely oxidized to NO_3^-: NO_2^- was converted to NO_3^- by the following reaction:

$$NO_2^- + 0.5O_2 \rightarrow NO_3^- \quad (2)$$

The pH of the effluent was stable around 6.2 at the later period of phase 4. To increase the effluent pH value, the pH of the influent medium was changed to 7.5 in phase 5. As a result, the effluent pH slightly increased to 6.3–6.5. However, no apparent Mn removal was observed at the end of phase 5. Because it was also expected that a high concentration of Mn(II) could inhibit the enrichment of Mn(II)-oxidizing microbial populations, the Mn(II) concentration in the influent medium was reduced in phase 6. Although reactor A was operated for 161 days in phase 6, Mn removal and blackish precipitations indicative of Mn oxides were not observed. In phase 7, the HRT was returned to 4.5 hours to extend the reaction time with the microbial cells and Mn(II). The oxidation of NH_4^+ to NO_3^- was continuously observed during phases 5 to 7. However, the production of BioMnOx was not observed during the operation of reactor A for 636 days. Therefore, we abandoned the production of Mn oxides using reactor A.

Operation of DHS bioreactor supplemented with CH_4 (reactor M)

In parallel to reactor A, we ran another DHS reactor that was supplemented with CH_4 as the alternative energy source (named reactor M). For this reactor, we added NH_4^+ and NO_3^- into the medium as nitrogen sources. After the first 10 days in phase 1, Mn^{2+} removal was observed (Figure 2), but it might be due to adsorption to sponges and/or inoculated cells (although this phenomenon was not observed in reactor A). At the end of phase 1, NO_2^- production accompanied with NH_4^+ oxidation was observed, and the pH value of the effluent decreased to 6.3 due to Reaction (1) as described above (Figure 2). In phase 2, the NH_4^+ concentration in the influent medium was reduced to

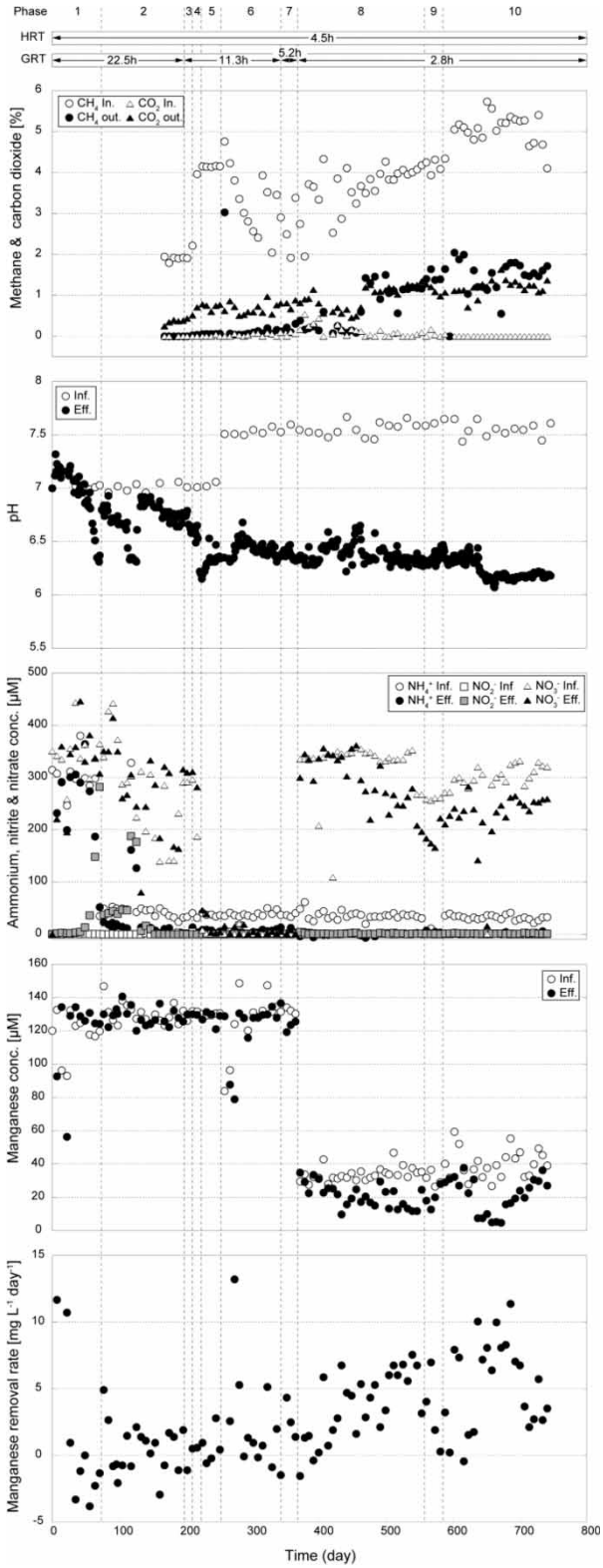

Figure 2 | Time courses of the proportions of CH_4 and CO_2 in the input gas and off-gas, pH, and concentrations of NH_4^+, NO_2^-, NO_3^-, and Mn^{2+} in the influent and effluent during the operation of reactor M. Mn(II) removal rates are also shown in the bottom panel, which were calculated from the Mn^{2+} concentrations.

one-tenth of the original concentration to avoid rapid acidification. At the later period of phase 2, NO_2^- was not detected in the effluent (Figure 2). The production of NO_2^- from NH_4^+ might decrease and the produced NO_2^- was converted to NO_3^- because the concentrations of NO_3^- in the effluent were higher than those in the influent. Measurements of the CH_4 concentration in the input and output gases were started at the later period of phase 2. The CH_4 in the input gas and off-gas was consumed probably due to the following reaction of methane oxidation:

$$CH_4 + 2O_2 \rightarrow CO_2 + 2H_2O \quad (3)$$

In fact, an elevated CO_2 concentration was observed in the off-gas (Figure 2). The produced CO_2 was likely partially dissolved into the liquid medium in the reactor, which is consistent with the pH decrease observed. To enhance the production of organic compounds from methane oxidation, the GRT was shortened, and the partial pressure of CH_4 in the input-gas was increased (from 2% to 4%) in the phases 3 to 5. Because NO_3^- did not seem to be utilized as the nitrogen source of the microbial community, the NO_3^- addition to the influent medium was stopped in phases 5 and 6. At the later period of phase 5, the pH was stable at 6.3. The decrease in the NH_4^+ concentration in the effluent was probably due to microbial uptake and assimilation because there was very little production of NO_2^- and NO_3^-. In phase 6, the pH of the influent medium was increased to 7.5. The pH of the effluent was slightly increased to 6.4–6.5. CH_4 consumption was continuously observed, but Mn(II) removal was not observed. It is unclear why a transient removal of Mn(II) was observed just after the start of phase 6 (Figure 2). Furthermore, when the GRT was more shortened in phase 7, Mn(II) removal was not observed.

Because the high concentration of Mn(II) was presumed to be inhibitory to the development of Mn(II)-oxidizing microbial populations, the Mn(II) concentration in the influent medium was reduced from 118 to 27 μM in phase 8. NO_3^- was added again to the medium as a nitrogen source, and the GRT was reduced in phase 8. Finally, Mn(II) removal was evident during phase 8 (Figure 2), and the color of the sponges gradually became blackish (Figure 1). These findings strongly suggested the occurrence of BioMnOx production in the bioreactor. The rate of Mn removal was continuously positive (average, 3.6 mg L^{-1} day^{-1}; maximum, 7.6 mg L^{-1} day^{-1}; Figures 2 and 3). In phase 9, the NH_4^+ addition to the influent medium was stopped to assess the effect of NH_4^+ on the Mn removal rate. As a result, the Mn removal rate slightly decreased (average, 3.3 mg L^{-1} day^{-1}; maximum, 7.0 mg L^{-1} day^{-1}), suggesting that NH_4^+ is important for BioMnOx production (potentially as the nitrogen source for Mn oxidizers). In phase 10, the NH_4^+ addition to the influent medium was resumed, and the Mn removal rate increased (average, 5.4 mg L^{-1} day^{-1}; maximum, 11.4 mg L^{-1} day^{-1}). The Mn removal rates observed in the reactor M are slower than that of the previous freshwater operation (constantly over 20 mg L^{-1} day^{-1}; maximum, 48 mg L^{-1} day^{-1}) (Cao *et al.* 2015).

Once Mn oxides are produced by Mn-oxidizing populations, organic radicals created by the Mn oxide-catalyzed oxidation can lead to the acceleration of Mn oxidation (i.e., Mn^{2+} removal from water) as discussed in a previous report (Learman *et al.* 2011b). In fact, the Mn removal rate in reactor M increased from phase 8 to phase 10 under the same experimental conditions (Figure 3). The organics for Mn oxide-catalyzed oxidation can be produced by the methanotroph-based microbial community because the influent medium lacks organic compounds. Therefore, it could be concluded that the Mn(II) oxidation in the bioreactor was driven by the microbial methane oxidation. It should be noted that aerobic conditions were maintained in the reactor during the Mn oxidation in the phases 8 to 10, i.e., the O_2 concentrations in the off-gas were between 10.2% and 19.8% (average 13.3%, $n = 271$). It is another possibility that the population of Mn(II)-oxidizing bacteria increased gradually during the phases and the occurrence of microbial enrichment caused the increase in Mn(II) oxidation rate. In either case, further analyses are needed to determine what led to the acceleration of Mn oxidation in reactor M.

Identification of Mn oxides using XRD analysis

To confirm whether the blackish materials formed in reactor M were Mn oxides or not, we analyzed the materials using an XRD analyzer. The XRD pattern (Figure 4) showed that the blackish particles were birnessite. Birnessite is a phyllomanganate consisting of sheets of edge-sharing MnO_6 octahedra, and their stacking is in the c-direction, yielding peaks at 2.4, 1.4, and ~7 Å, respectively (Villalobos *et al.* 2003, 2006). Specifically, the obtained XRD pattern was consistent with those of the BioMnOx products of known Mn-oxidizing bacteria, such as *Bacillus* sp. SG-1 (Bargar *et al.* 2005), *Pseudomonas putida* MnB1 (Villalobos *et al.* 2003, 2006), *Leptothrix discophora* SP-6 (Jürgensen *et al.* 2004), and *Roseobacter* sp. AzwK-3b (Learman *et al.* 2013). The broad peak observed at ~3.8 Å maybe

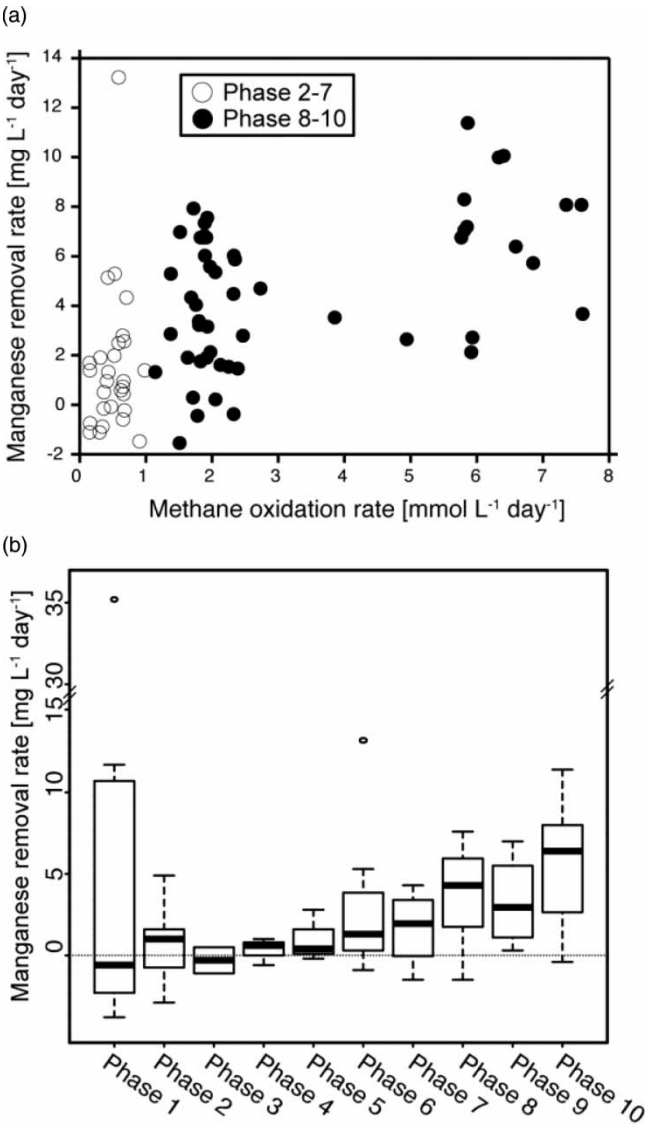

Figure 3 | Mn(II) removal rates during the operation of bioreactor M. (a) Mn(II) removal rates in relation to the methane-oxidation rate. (b) Box plot of the Mn removal rates for the bioreactor operation.

originated from microbial cell materials as shown in previous studies (Jürgensen *et al.* 2004; Villalobos *et al.* 2006). BioMnOx can transform to 10 Å triclinic phyllomanganate, and then to todorokite, which have been shown by laboratory experiments using cultures of a Mn(II)-oxidizing bacterium, *Pseudomonas putida* strain GB-1 (Feng *et al.* 2010). However, despite the long-term operation, the typical peaks for 10 Å triclinic phyllomanganate and todorokite were not observed in the present study. This might be due to the difference in experimental conditions between the previous study (Feng *et al.* 2010) and the present study, such as microbial source (isolate vs. community), cultivation type (batch vs. continuous flow) and medium (freshwater vs. seawater).

Composition of the microbial community in the inoculum sample

We determined the 16S rRNA gene phylotype composition of the original inoculum to assess the shift in the microbial community during the reactor operations. The results of the 16S rRNA gene-based clone analysis are summarized in Figure 5 and Table 2, and the phylogenetic positions of the representative OTUs are shown in Figures S3–S7 (available with the online version of this paper).

The OTUs classified in *Deltaproteobacteria* (putative sulfate/metal reducers) and in *Zetaproteobacteria* (putative iron oxidizers) were the first and second most abundant in the bacterial clone library, respectively. The OTUs classified in *Methylococcales* of *Gammaproteobacteria* (putative methanotrophs) were also relatively abundant. The OTUs classified in *Nitrospirae* and *Nitrospinae* (both putative nitrite oxidizers) and *Nitrosomonadales* of *Betaproteobacteria* (putative ammonia oxidizers) were detected. OTUs classified in *Planctomycetes*, *Alphaproteobacteria*, and *Gammaproteobacteria* (putative heterotrophs) were also detected. An OTU related to *Nitrosopumilus* spp. in *Thaumarchaeota* (putative ammonia oxidizers) dominated in the archaeal clone library. The bacterial 16S rRNA gene phylotype composition in the original inoculum was quite different from those of the microbial communities colonizing sponges collected during the operation (Figure 5(a), as supported by the comparative analysis (Figure 5(b)). Remarkably, only one OTU (OTUb17 in *Nitrospinae*) in the original inoculum (OriB) was found in the bacterial phylotype compositions during the operation of reactor A (ATB, AMB and ABB), and no OTU of OriB was found in the bacterial phylotype composition in reactor M (MTB and MBB) (Figure 5(c)). The results indicate that the bacterial populations represented by the OTUs during the reactor operation were not just a remnant of the inoculum, but actively grew in the reactors.

Microbial community composition in reactor A

At day 532, we collected the top, middle and bottom parts of the string of the sponges and determined the bacterial and archaeal community compositions (Figure 5(a)). An OTU classified in *Nitrosomonadales* of *Betaproteobacteria*, OTUb84, was the most abundant in the bacterial clone libraries for all parts (ATB, AMB, and ABB) (Figure S3).

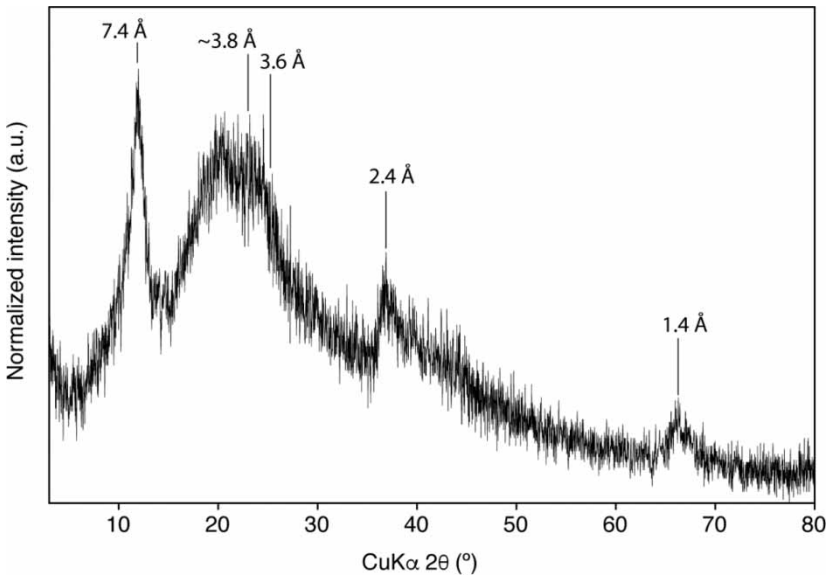

Figure 4 | XRD pattern of BioMnOx.

This OTU was closely related to ammonia-oxidizing autotrophic bacteria, such as *Nitrosomonas* spp. and *Nitrosococcus* spp. OTUb86 in *Nitrospinae* was also relatively abundant in the libraries (Figure S5). One OTU (OTUa1) related to an ammonia-oxidizing archaeon, *Nitrosopumilus maritimus*, was recovered from the archaeal clone libraries constructed from the middle and bottom parts (AMA and ABA) in reactor A. These OTUs related to *Nitrosomonadales*, *Nitrospinae* and *Nitrosopumilus* likely represent ammonia/nitrite oxidizers, and contribute to Reactions (1) and (2), respectively, observed in reactor A as described above. In addition, these putative autotrophs likely fix inorganic carbon into organic carbon and support the growth of heterotrophs in the reactor as the primary producers.

OTUs classified in *Bacteroidetes*, *Phycisphaerales* of *Planctomycetes*, and *Kiloniellales* and *Rhodobacterales* of *Alphaproteobacteria* (Figures S4–S6), which likely represent heterotrophs, were relatively abundant in the libraries (3.0–12.9% of the total number of clones) for all parts. These putative heterotrophs would use the organic carbon produced by the autotrophic ammonia/nitrite oxidizers as described above. To date, diverse heterotrophic Mn-oxidizing bacteria including members of *Rhodobacterales* and *Pseudomonadales* have been reported (Tebo *et al.* 2005; Templeton *et al.* 2005). However, all the sequences of *Rhodobacterales* and *Pseudomonadales* OTUs found in reactor A were distinct from those of previously known Mn-oxidizing bacteria (Figures S3 and S4). In addition, it is difficult to infer the ability of Mn oxidation from 16S rRNA gene sequence information because the ability is not common even among the same genus and/or species (for example, *Pseudomonas* species in Figure S3 (Francis & Tebo 2001)). Combined with the fact that no Mn removal was observed in reactor A after the long-term cultivation with various operational conditions, the host microorganisms of *Rhodobacterales* and *Pseudomonadales* OTUs are probably not Mn-oxidizing bacteria.

In the previous study, BioMnOx production was observed using a DHS reactor under freshwater conditions (total of 449 days of operation) (Cao *et al.* 2015), but in the present study, BioMnOx production was not observed in reactor A under the seawater conditions (total of 636 days), although NH_4^+ was used as the sole energy source for both reactors. The microbial communities were clearly different between the previous freshwater and the present seawater conditions (Figure 5(a) and (b)). No OTU was common between the freshwater and seawater reactors (Figure 5(c)). The difference in the microbial community development is due to the different inoculum sources and enrichment conditions, which ultimately led to the unsuccessful BioMnOx production in our DHS reactor under the marine conditions.

Microbial community composition in reactor M

At day 634, the top and bottom parts of the string of sponges were collected, and the bacterial and archaeal community compositions were determined (Figure 5(a)). The bacterial

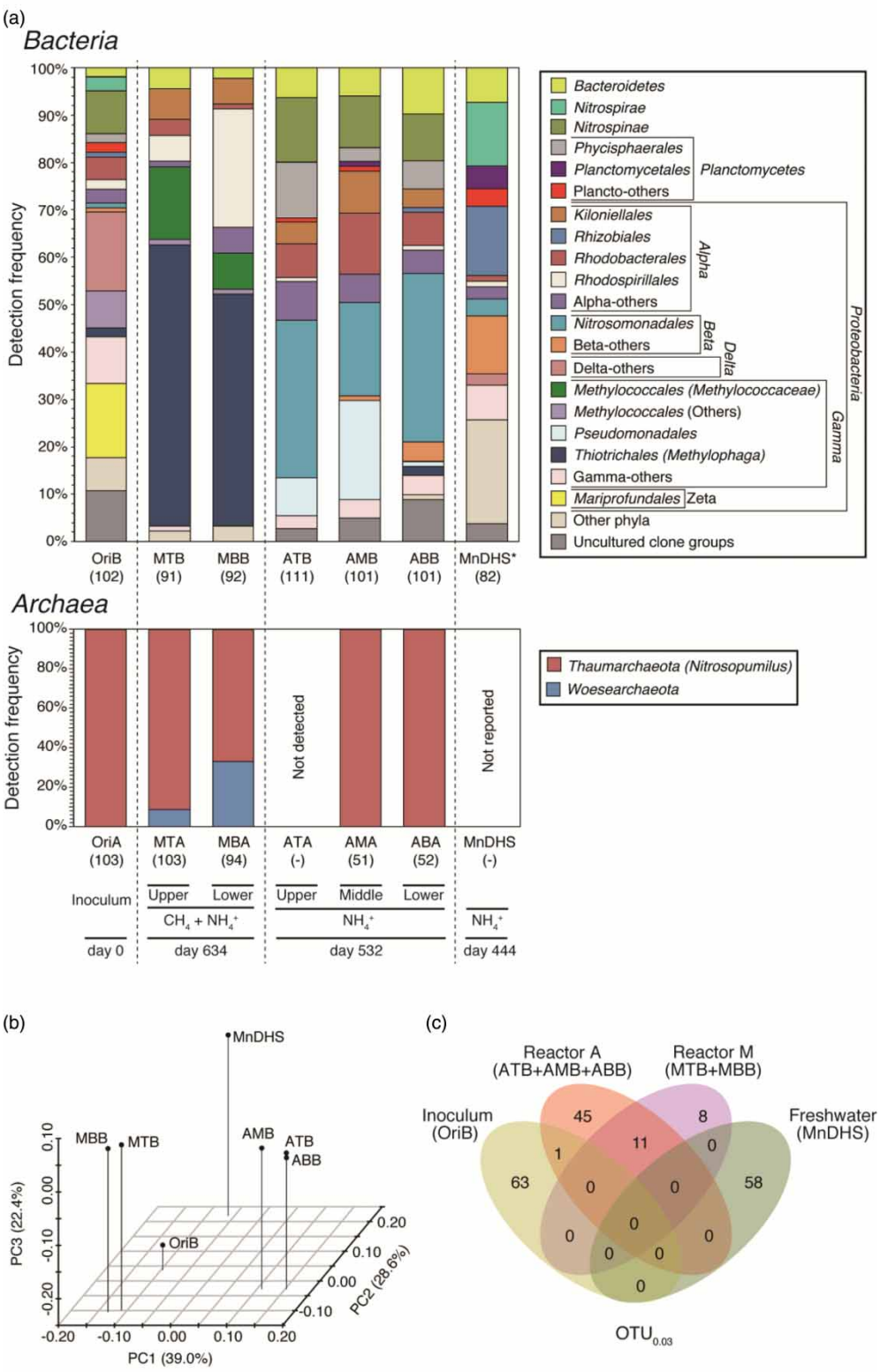

Figure 5 | Microbial community structures in reactors A and M based on 16S rRNA gene clone library analyses. (a) Bacterial and archaeal community structures. Numbers of analyzed clones are indicated in parentheses. (b) Comparison of the bacterial community structures by principal coordinate analysis with the UniFrac weighted method. (c) Venn diagram showing the numbers of unique and common OTUs among bacterial communities in the inoculum, reactors A and M, and freshwater reactor (MnDHS). Data for MnDHS are from previous report (Cao *et al.* 2015).

Table 2 | Summary of the Q-PCR and PCR clone library analyses

Sample		Target taxa	Sample ID	Q-PCR analysis: Copy number (copies/g)	Q-PCR analysis: Estimated cell number (cells/g)	PCR clone library analysis: Number of total clones	PCR clone library analysis: Number of OTUs	PCR clone library analysis: Coverage
Inoculum		*Bacteria*	OriB	N.A.[a]	N.A.	102	64	54.9%
		Archaea	OriA	N.A.	N.A.	103	1	100%
Reactor M	Top	*Bacteria*	MTB	$1.9\ (\pm0.49)\times10^{10}$	$4.6\ (\pm0.12)\times10^{9}$	91	14	91.2%
		Archaea	MTA	$1.6\ (\pm0.06)\times10^{8}$	$9.8\ (\pm0.04)\times10^{7}$	103	2	100%
	Bottom	*Bacteria*	MBB	$1.3\ (\pm0.11)\times10^{10}$	$3.2\ (\pm0.03)\times10^{9}$	92	12	95.7%
		Archaea	MBA	$1.5\ (\pm0.35)\times10^{7}$	$9.2\ (\pm0.21)\times10^{6}$	94	3	100%
Reactor A	Top	*Bacteria*	ATB	$1.6\ (\pm0.04)\times10^{11}$	$3.9\ (\pm0.01)\times10^{10}$	111	27	85.6%
		Archaea	ATA	N.D.[b]	N.D.	N.D.	N.D.	N.A.
	Middle	*Bacteria*	AMB	$2.2\ (\pm0.08)\times10^{10}$	$5.3\ (\pm0.02)\times10^{9}$	101	33	81.2%
		Archaea	AMA	N.D.	N.D.	51	1	100%
	Bottom	*Bacteria*	ABB	$1.6\ (\pm0.06)\times10^{8}$	$3.9\ (\pm0.01)\times10^{7}$	101	36	75.8%
		Archaea	ABA	N.D.	N.D.	52	1	100%
Freshwater[c]		*Bacteria*	MnDHS	N.R.[d]	N.R.	82	58	41.5%

[a]Not analyzed.
[b]Not detected.
[c]Data from Cao *et al*. (2015).
[d]Not reported.

communities of reactor M were clearly different from those of reactor A and the original inoculum (Figure 5). The colonization of microorganisms was confirmed by SEM, showing that the vacancies in the sponges were filled with dense microbial populations and extracellular nano-wire-like structures (Figure 6). The SEM observations are consistent with the high cell numbers in the sponges estimated by Q-PCR (Table 2).

An OTU classified in *Thiotrichales* of *Gammaproteobacteria*, OTUb87, was the most abundant (>50% of the total number of clones for each library) in the bacterial libraries (MTB and MBB) of reactor M. The closest cultured species to the OTUb87, with <95% of the 16S rRNA gene sequence similarity, was *Methylophaga* spp., which are methylotrophs that use one-carbon compounds (e.g., methanol, formaldehyde, and methylamine) except methane as their sole carbon and energy sources (Lidstrom 2006). Considering its relative abundance and the incubation conditions of reactor M, the host bacterium of OTUb87 can be regarded as a methanotroph. However, the same sequence was found in reactor A and no cultured methanotroph species have been reported in *Thiotrichales*. Therefore, the host bacterium may use methanol provided by other methanotrophs as described below.

An OTU classified in *Methylococcaceae* of *Gammaproteobacteria*, OTUb118, was relatively abundant in the libraries. The closest cultured species to the OTUb118, with 98% of the 16S rRNA gene sequence similarity, was *Methylomonas* spp., which are methanotrophs that use methane and methanol as the sole carbon and energy sources (Bowman 2015). Thus, the host bacterium of OTUb118 could be a methanotroph, which could grow in reactor M using methane and sustain the other concomitant other heterotrophs including Mn oxidizers as a primary producer. No sequences related to methanotrophs were detected in reactor A.

An OTU classified in *Rhodospirillales* of *Alphaproteobacteria*, OTUb115, was relatively abundant (5.5%–25.0% of the total number of clones) in the libraries of reactor M but was rarely detected in reactor A (Figure S4). The closest cultured species to the OTUb115, with 99% of the 16S rRNA gene sequence similarity, was *Nisaea* spp., which are heterotrophs including facultative anaerobes. As observed in reactor A, OTUs classified in *Bacteroidetes*, and *Kiloniellales* and *Rhodobacterales* of *Alphaproteobacteria*, which likely represent heterotrophs, were also detected in the libraries for reactor M (1.1%–6.4% of the total number of clones). The putative heterotrophs of these OTUs can grow using the organic compounds from the methanotrophic primary producers. In contrast, OTUs in *Nitrosomonadales* of *Betaproteobacteria* (putative ammonia oxidizers) and in *Nitrospinae* (putative nitrite oxidizers) were not detected in reactor M. These results indicate that in reactor M, the methanotrophic populations overcame the populations of ammonium oxidizers, and NH_4^+ in the medium was preferentially consumed, probably by the

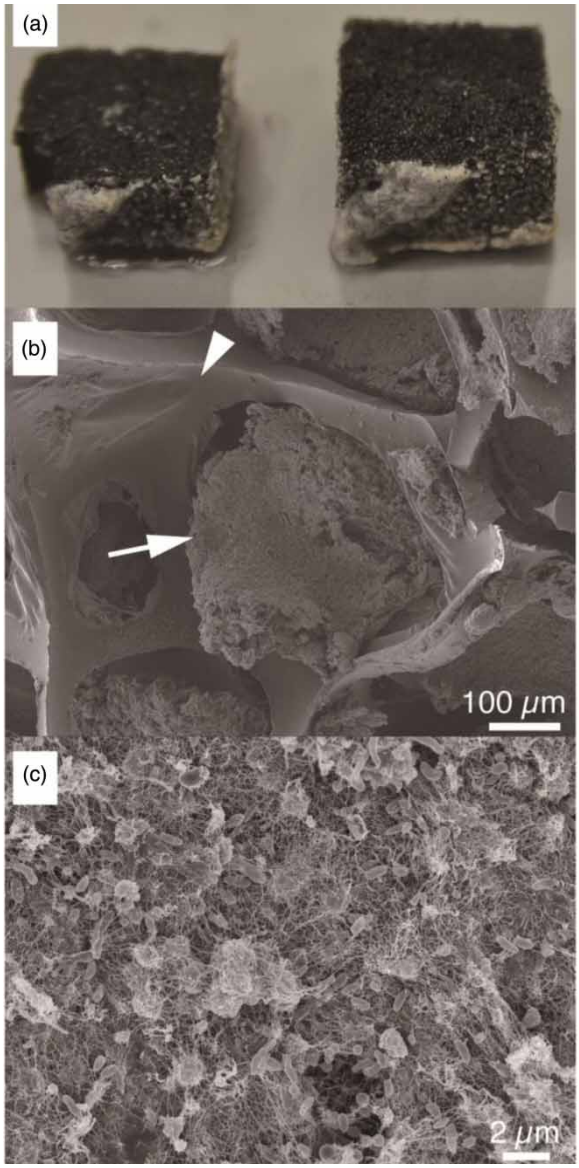

Figure 6 | (a) Photograph of a sponge cut in half, which was collected on day 634. Whitish microbial mats were observed on the sponge. The sponge size is 2 × 2 × 2 cm. (b) SEM image of the sponge on day 634 at a magnification of ×150. Vacancies in the sponge were filled with microbial flocs, as shown by white arrow. The frame of the sponge is indicated with a white arrowhead. (c) SEM image at a magnification of ×5,000. Dense cocci- and rod-shaped microbes with numerous nano-sized fibers can be seen.

nitrogen assimilation, by abundant methano/methylotrophic and heterotrophic populations rather than by the dissimilatory nitrogen metabolism of nitrifiers, which is consistent with the chemical data (Figure 2).

OTUa1 related to the ammonium-oxidizing archaeon *Nitrosopumilus maritimus* was the most abundant in the archaeal 16S rRNA gene clone libraries. The archaeal 16S rRNA gene abundance was estimated to account for 0.3–2.1% of the total number of cells in reactor M (Table 2), indicating that the detected archaeal members could actively grow in the reactor and represent a portion of the microbial community. Thus, it can be concluded that bacterial populations including methanotrophs predominated in reactor M.

Phylogenetically diverse microorganisms were detected from reactor M. However, we could not identify Mn-oxidizing bacteria because identical or very close to 16S rRNA gene sequences of previously known Mn-oxidizing bacteria were not detected from the reactor. Therefore, at present, it is still uncertain which of the OTUs and their host microbes are responsible for the BioMnOx production in reactor M. To date, phylogenetically diverse bacteria have been shown to be capable of Mn oxidation by means of indigenous Mn-oxidizing enzymes or metabolic superoxides. Enzymatic Mn oxidation has been demonstrated in several bacteria, such as *Bacillus* spp. (*Firmicutes*), *Pseudomonas* spp. (*Gammaproteobacteria*), *Arthrobacter* spp. (*Actinobacteria*), and *Leptothrix* spp. (*Betaproteobacteria*) (Tebo *et al.* 2005). Mn oxidation by superoxides has been shown in *Roseobacter* spp. (*Alphaproteobacteria*) (Learman *et al.* 2011a). A recent report showed that diverse bacteria in various environments, including marine environments, can produce extracellular superoxides (Diaz *et al.* 2013), which can oxidize circumambient Mn. In addition, phylogenetically diverse Mn-oxidizing bacteria, such as *Roseobacter* spp. and *Sulfitobacter* spp. (*Alphaproteobacteria*), as well as *Pseudoalteromonas* spp. and *Alteromonas* spp. (*Gammaproteobacteria*), have been isolated from deep-sea basaltic rocks, although the mechanisms of their Mn oxidation are unclear (Templeton *et al.* 2005). Considering the presence of the phylogenetically diverse Mn-oxidizing bacteria, it is not surprising that there are yet-unknown Mn oxidizers in reactor M. Indeed, we could not exclude the possibility that undetected microorganisms are involved in the BioMnOx production, as the coverage values of the 16S rRNA gene clone analyses (Table 2) indicate the presence of undetected microbial populations in the microbial community of reactor M.

The bacterial communities found in reactor M (and also reactor A) were totally different from those of the previously described freshwater reactor (Cao *et al.* 2015). No common OTUs were found between the microbial communities (Figure 5(c)). This result indicates that the Mn-oxidizing population enriched in our seawater reactor differ from that in the freshwater reactor. The difference in salinity between the marine and freshwater reactors, in addition to the differences in inoculum source (deep-sea sediment vs.

activated sludge) and the availability of CH_4, likely results in the difference in the microbial community structures. It should be noted that microorganisms responsible for BioMnOx in the previously described freshwater reactor are also unclear (Cao *et al.* 2015) as in the present study.

CONCLUSION

In this study, we successfully achieved Mn removal and Mn oxides production under the marine conditions by coupling with methane oxidation during the operation of reactor M. Although the detailed mechanism of Mn oxides production in reactor M is still unclear, our data strongly indicated that Mn oxides were produced by microorganisms in reactor M as supported by the following reasons: (i) positive correlation was found between manganese removal rate and methane-oxidation rate (Figure 3) and (ii) XRD analysis showed that blackish material formed in reactor M has a very similar pattern to birnessite that is normally produced by previously known Mn-oxidizing bacteria (Figure 4). Based on comparisons of the operation of reactors A and M, certain organic compounds produced by methanotrophs may activate yet-unknown Mn-oxidizing microbial populations, whereas the compounds produced by nitrifiers from the deep-sea sediment sample in the seawater reactor may not activate them, even though a freshwater DHS reactor was previously successfully shown to produce the BioMnOx with nitrification (Cao *et al.* 2015). Otherwise, methanotrophs themselves may oxidize Mn in reactor M, although we obtained no clear evidence to support this hypothesis. Further attempt at cultivation of Mn oxidizers from the reactor and the biochemical analysis of isolates will clarify which microbial components are responsible for the observed Mn oxidation and how the Mn oxidation is linked to methane oxidation. In the future, we will develop more effective continuous-flow bioreactor systems, with higher Mn removal rates, containing various marine microbial communities and demonstrate their adsorptive properties for the recovery of trace metals and their possible applications in engineering.

ACKNOWLEDGEMENTS

Shingo Kato and Masayuki Miyazaki contributed equally to this work. The authors would like to thank Katsuyuki Uematsu and Akihiro Tame for assistance in preparing the electron micrographs. We are very grateful to the ROV *Hyper-Dolphin* operation team and the crew of the R/V *Natsushima*, and Dr Hiroko Makita for helping us to collect the deep-sea sample. This study was supported by the Japan Society for the Promotion of Science (JSPS) KAKENHI grants (no. 24561008 to author M. M., no. 24687011 and 15H02419 to author H. I.) and by the Cabinet Office, Government of Japan, through the 'next-generation technology for ocean resources exploration' (called as Zipangu-in-the-ocean project) in the Cross-ministerial Strategic Innovation Promotion Program. The authors have no conflict of interest to declare.

REFERENCES

Aoki, M., Ehara, M., Saito, Y., Yoshioka, H., Miyazaki, M., Saito, Y., Miyashita, A., Kawakami, S., Yamaguchi, T., Ohashi, A., Nunoura, T., Takai, K. & Imachi, H. 2014 A long-term cultivation of an anaerobic methane-oxidizing microbial community from deep-sea methane-seep sediment using a continuous-flow bioreactor. *PLoS ONE* **9** (8), e105356.

Bargar, J. R., Tebo, B. M., Bergmann, U., Webb, S. M., Glatzel, P., Chiu, V. Q. & Villalobos, M. 2005 Biotic and abiotic products of Mn(II) oxidation by spores of the marine *Bacillus* sp. strain SG-1. *American Mineralogist* **90** (1), 143–154.

Bowman, J. P. 2015 *Methylomonas*. In: *Bergey's Manual of Systematics of Archaea and Bacteria*. Wiley, New York.

Cao, L. T. T., Kodera, H., Abe, K., Imachi, H., Aoi, Y., Kindaichi, T., Ozaki, N. & Ohashi, A. 2015 Biological oxidation of Mn(II) coupled with nitrification for removal and recovery of minor metals by downflow hanging sponge reactor. *Water Research* **68**, 545–553.

Capella-Gutierrez, S., Silla-Martinez, J. M. & Gabaldon, T. 2009 Trimal: a tool for automated alignment trimming in large-scale phylogenetic analyses. *Bioinformatics* **25** (15), 1972–1973.

Caporaso, J. G., Kuczynski, J., Stombaugh, J., Bittinger, K., Bushman, F. D., Costello, E. K., Fierer, N., Pena, A. G., Goodrich, J. K., Gordon, J. I., Huttley, G. A., Kelley, S. T., Knights, D., Koenig, J. E., Ley, R. E., Lozupone, C. A., Mcdonald, D., Muegge, B. D., Pirrung, M., Reeder, J., Sevinsky, J. R., Turnbaugh, P. J., Walters, W. A., Widmann, J., Yatsunenko, T., Zaneveld, J. & Knight, R. 2010 QIIME allows analysis of high-throughput community sequencing data. *Nature Methods* **7** (5), 335–336.

Diallo, M. S., Kotte, M. R. & Cho, M. 2015 Mining critical metals and elements from seawater: opportunities and challenges. *Environmental Science & Technology* **49** (16), 9390–9399.

Diaz, J. M., Hansel, C. M., Voelker, B. M., Mendes, C. M., Andeer, P. F. & Zhang, T. 2013 Widespread production of extracellular superoxide by heterotrophic bacteria. *Science* **340** (6137), 1223–1226.

Dick, G. J., Torpey, J. W., Beveridge, T. J. & Tebo, B. M. 2008 Direct identification of a bacterial manganese(II) oxidase, the multicopper oxidase MnxG, from spores of several different

marine *Bacillus* species. *Applied and Environmental Microbiology* **74** (5), 1527–1534.

Dixon, J. & Skinner, H. 1992 Manganese minerals in surface environments. In: *Biomineralization Processes of Iron and Manganese: Modern and Ancient Environments* (H. C. W. Skinner & R. W. Fitzpatrick, eds), Catena Verlag, Cremlingen-Destedt, Germany, pp. 31–50.

Edgar, R. C. 2004 MUSCLE: multiple sequence alignment with high accuracy and high throughput. *Nucleic Acids Research* **32** (5), 1792–1797.

Feng, X. H., Zhu, M., Ginder-Vogel, M., Ni, C., Parikh, S. J. & Sparks, D. L. 2010 Formation of nano-crystalline todorokite from biogenic Mn oxides. *Geochimica et Cosmochimica Acta* **74** (11), 3232–3245.

Francis, C. A. & Tebo, B. M. 2001 *cumA* multicopper oxidase genes from diverse Mn(II)-oxidizing and non-Mn(II)-oxidizing *Pseudomonas* strains. *Applied and Environmental Microbiology* **67** (9), 4272–4278.

Glasby, G. 2006 Manganese: predominant role of nodules and crusts. In: *Marine Geochemistry* (H. Schulz & M. Zabel, eds). Springer, Berlin, pp. 371–427.

Hallberg, K. B. & Johnson, D. B. 2005 Biological manganese removal from acid mine drainage in constructed wetlands and prototype bioreactors. *Science of the Total Environment* **338** (1–2), 115–124.

Hansel, C. M., Zeiner, C. A., Santelli, C. M. & Webb, S. M. 2012 Mn(II) oxidation by an ascomycete fungus is linked to superoxide production during asexual reproduction. *Proceedings of the National Academy of Sciences of the United States of America* **109** (31), 12621–12625.

Hein, J. R., Mizell, K., Koschinsky, A. & Conrad, T. A. 2013 Deep-ocean mineral deposits as a source of critical metals for high- and green-technology applications: comparison with land-based resources. *Ore Geology Reviews* **51**, 1–14.

Hennebel, T., De Gusseme, B., Boon, N. & Verstraete, W. 2009 Biogenic metals in advanced water treatment. *Trends in Biotechnology* **27** (2), 90–98.

Hochella, M. F., Lower, S. K., Maurice, P. A., Penn, R. L., Sahai, N., Sparks, D. L. & Twining, B. S. 2008 Nanominerals, mineral nanoparticles, and earth systems. *Science* **319** (5870), 1631–1635.

Imachi, H., Aoi, K., Tasumi, E., Saito, Y., Yamanaka, Y., Saito, Y., Yamaguchi, T., Tomaru, H., Takeuchi, R., Morono, Y., Inagaki, F. & Takai, K. 2011 Cultivation of methanogenic community from subseafloor sediments using a continuous-flow bioreactor. *The ISME Journal* **5** (12), 1913–1925.

Jürgensen, A., Widmeyer, J. R., Gordon, R. A., Bendell-Young, L. I., Moore, M. M. & Crozier, E. D. 2004 The structure of the manganese oxide on the sheath of the bacterium *Leptothrix discophora*: an XAFS study. *American Mineralogist* **89** (7), 1110–1118.

Kashiwabara, T., Takahashi, Y., Tanimizu, M. & Usui, A. 2011 Molecular-scale mechanisms of distribution and isotopic fractionation of molybdenum between seawater and ferromanganese oxides. *Geochimica et Cosmochimica Acta* **75** (19), 5762–5784.

Kashiwabara, T., Takahashi, Y., Marcus, M. A., Uruga, T., Tanida, H., Terada, Y. & Usui, A. 2013 Tungsten species in natural ferromanganese oxides related to its different behavior from molybdenum in oxic ocean. *Geochimica et Cosmochimica Acta* **106**, 364–378.

Kashiwabara, T., Oishi, Y., Sakaguchi, A., Sugiyama, T., Usui, A. & Takahashi, Y. 2014 Chemical processes for the extreme enrichment of tellurium into marine ferromanganese oxides. *Geochimica et Cosmochimica Acta* **131**, 150–163.

Learman, D. R., Voelker, B. M., Vazquez-Rodriguez, A. I. & Hansel, C. M. 2011a Formation of manganese oxides by bacterially generated superoxide. *Nature Geoscience* **4** (2), 95–98.

Learman, D. R., Wankel, S. D., Webb, S. M., Martinez, N., Madden, A. S. & Hansel, C. M. 2011b Coupled biotic–abiotic Mn(II) oxidation pathway mediates the formation and structural evolution of biogenic Mn oxides. *Geochimica et Cosmochimica Acta* **75** (20), 6048–6063.

Learman, D. R., Voelker, B. M., Madden, A. S. & Hansel, C. M. 2013 Constraints on superoxide mediated formation of manganese oxides. *Frontiers in Microbiology* **4**, 262.

Lidstrom, M. E. 2006 Aerobic methylotrophic prokaryotes. In: *The Prokaryotes* (M. Dworkin, S. Falkow, E. Rosenberg, K.-H. Schleifer & E. Stackebrandt, eds). Springer, New York, pp. 618–634.

Makita, H., Kikuchi, S., Mitsunobu, S., Takaki, Y., Yamanaka, T., Toki, T., Noguchi, T., Nakamura, K., Abe, M., Hirai, M., Yamamoto, M., Uematsu, K., Miyazaki, J., Nunoura, T., Takahashi, Y. & Takai, K. 2016 Comparative analysis of microbial communities in iron-dominated flocculent mats in deep-sea hydrothermal environments. *Applied and Environmental Microbiology* **82** (19), 5741–5755.

Manceau, A., Charlet, L., Boisset, M., Didier, B. & Spadini, L. 1992 Sorption and speciation of heavy metals on Fe and Mn hydrous oxides from microscopic to macroscopic. *Applied Clay Science* **7** (1–3), 201–223.

Maruo, M., Doi, T. & Obata, H. 2006 Onboard determination of submicromolar nitrate in seawater by anion-exchange chromatography with lithium chloride eluent. *Analytical Sciences* **22** (9), 1175–1178.

Miyata, N., Tani, Y., Maruo, K., Tsuno, H., Sakata, M. & Iwahori, K. 2006 Manganese(IV) oxide production by *Acremonium* sp. strain kr21-2 and extracellular Mn(II) oxidase activity. *Applied and Environmental Microbiology* **72** (10), 6467–6473.

Miyata, N., Tani, Y., Sakata, M. & Iwahori, K. 2007 Microbial manganese oxide formation and interaction with toxic metal ions. *Journal of Bioscience and Bioengineering* **104** (1), 1–8.

Myers, C. R. & Nealson, K. H. 1988 Bacterial manganese reduction and growth with manganese oxide as the sole electron acceptor. *Science* **240** (4857), 1319–1321.

Post, J. E. 1999 Manganese oxide minerals: crystal structures and economic and environmental significance. *Proceedings of the National Academy of Sciences of the United States of America* **96** (7), 3447–3454.

Price, M. N., Dehal, P. S. & Arkin, A. P. 2010 FastTree 2–approximately maximum-likelihood trees for large alignments. *PLoS ONE* **5** (3), e9490.

Santelli, C. M., Webb, S. M., Dohnalkova, A. C. & Hansel, C. M. 2011 Diversity of Mn oxides produced by Mn(II)-oxidizing

fungi. *Geochimica et Cosmochimica Acta* **75** (10), 2762–2776.

Schloss, P. D., Westcott, S. L., Ryabin, T., Hall, J. R., Hartmann, M., Hollister, E. B., Lesniewski, R. A., Oakley, B. B., Parks, D. H., Robinson, C. J., Sahl, J. W., Stres, B., Thallinger, G. G., Van Horn, D. J. & Weber, C. F. 2009 Introducing mothur: open-source, platform-independent, community-supported software for describing and comparing microbial communities. *Applied and Environmental Microbiology* **75** (23), 7537–7541.

Sherman, D. M. & Peacock, C. L. 2010 Surface complexation of Cu on birnessite (δ-MnO_2): controls on Cu in the deep ocean. *Geochimica et Cosmochimica Acta* **74** (23), 6721–6730.

Stoddard, S. F., Smith, B. J., Hein, R., Roller, B. R. & Schmidt, T. M. 2015 rrnDB: improved tools for interpreting rRNA gene abundance in bacteria and archaea and a new foundation for future development. *Nucleic Acids Research* **43** (Database issue), D593–D598.

Takahashi, Y., Manceau, A., Geoffroy, N., Marcus, M. A. & Usui, A. 2007 Chemical and structural control of the partitioning of Co, Ce, and Pb in marine ferromanganese oxides. *Geochimica et Cosmochimica Acta* **71** (4), 984–1008.

Tebo, B. M., Bargar, J. R., Clement, B. G., Dick, G. J., Murray, K. J., Parker, D., Verity, R. & Webb, S. M. 2004 Biogenic manganese oxides: properties and mechanisms of formation. *Annual Review of Earth and Planetary Sciences* **32** (1), 287–328.

Tebo, B. M., Johnson, H. A., Mccarthy, J. K. & Templeton, A. S. 2005 Geomicrobiology of manganese(II) oxidation. *Trends in Microbiology* **13** (9), 421–428.

Tebo, B. M., Geszvain, K. & Lee, S.-W. 2010 The molecular geomicrobiology of bacterial manganese(II) oxidation. In: *Geomicrobiology: Molecular and Environmental Perspective* (L. L. Barton, M. Mandl & A. Loy, eds). Springer, Dordrecht, The Netherlands, pp. 285–308.

Templeton, A. S., Staudigel, H. & Tebo, B. M. 2005 Diverse Mn(II)-oxidizing bacteria isolated from submarine basalts at Loihi seamount. *Geomicrobiology Journal* **22** (3–4), 127–139.

Van Waasbergen, L. G., Hildebrand, M. & Tebo, B. M. 1996 Identification and characterization of a gene cluster involved in manganese oxidation by spores of the marine *Bacillus* sp. strain SG-1. *Journal of Bacteriology* **178** (12), 3517–3530.

Villalobos, M., Toner, B., Bargar, J. & Sposito, G. 2003 Characterization of the manganese oxide produced by *Pseudomonas putida* strain MnB1. *Geochimica et Cosmochimica Acta* **67** (14), 2649–2662.

Villalobos, M., Lanson, B., Manceau, A., Toner, B. & Sposito, G. 2006 Structural model for the biogenic Mn oxide produced by *Pseudomonas putida*. *American Mineralogist* **91** (4), 489–502.

Yamanaka, T., Nagashio, H., Nishio, R., Kondo, K., Noguchi, T., Okamura, K., Nunoura, T., Makita, H., Nakamura, K., Watanabe, H., Inoue, K., Toki, K., Tsunogai, U., Nakada, R., Ohshima, S., Toyoda, S., Kawai, J., Yoshida, N., Ijiri, A. & Sunamura, M. 2015 The Tarama knoll: geochemical and biological profiles of hydrothermal activity. In: *Subseafloor Biosphere Linked to Hydrothermal Systems: Taiga Concept* (J. Ishibashi, K. Okino, K & M. Sunamura, eds). Springer, Tokyo, Japan, pp. 497–504.

First received 27 December 2016; accepted in revised form 5 June 2017. Available online 19 June 2017